



TITLE:

New diagnostic method for Alzheimer's disease based on the toxic conformation theory of amyloid β

AUTHOR(S):

Irie, Kazuhiro

CITATION:

Irie, Kazuhiro. New diagnostic method for Alzheimer's disease based on the toxic conformation theory of amyloid β . *Bioscience, Biotechnology and Biochemistry* 2020, 84(1): 1-16

ISSUE DATE:

2020

URL:

<http://hdl.handle.net/2433/245866>

RIGHT:

This is an Accepted Manuscript of an article published by Taylor & Francis in *Bioscience, Biotechnology and Biochemistry* on 20 September 2019, available online: <http://www.tandfonline.com/10.1080/09168451.2019.1667222>.; The full-text file will be made open to the public on 20 September 2020 in accordance with publisher's 'Terms and Conditions for Self-Archiving'; この論文は出版社版ではありません。引用の際には出版社版をご確認ご利用ください。; This is not the published version. Please cite only the published version.

1 **New diagnostic method for Alzheimer's disease based on the toxic**
2 **conformation theory of amyloid β**

3

4 Kazuhiro Irie

5 *Division of Food Science and Biotechnology, Graduate School of Agriculture, Kyoto*

6 *University, Kyoto 606-8502, Japan*

7

8

9

10

11

12

13

14

15

16

17

18

19

20

21

22

23 CONTACT Kazuhiro Irie: irie@kais.kyoto-u.ac.jp

24 This review was written in response to the author's receipt of the Japan Society for
25 Bioscience, Biotechnology, and Agrochemistry Award in 2019.

26

27 **Abstract**

28 Recent investigations suggest that soluble oligomeric amyloid β ($A\beta$)
29 species may be involved in early onset of Alzheimer's disease (AD). Using
30 systematic proline replacement, solid-state NMR, and ESR, we identified a
31 toxic turn at position 22 and 23 of $A\beta$ 42, the most potent neurotoxic $A\beta$
32 species. Through radicalization, the toxic turn can induce formation of the
33 C-terminal hydrophobic core to obtain putative $A\beta$ 42 dimers and trimers.
34 Synthesized dimer and trimer models showed that the C-terminal
35 hydrophobic core plays a critical role in formation of high molecular weight
36 oligomers with neurotoxicity. Accordingly, an anti-toxic turn antibody
37 (24B3) that selectively recognizes a toxic dimer model of E22P- $A\beta$ 42 was
38 developed. Sandwich enzyme-linked immunosorbent assay with 24B3 and
39 82E1 detected a significantly higher ratio of $A\beta$ 42 with a toxic turn to total
40 $A\beta$ 42 in cerebrospinal fluid of AD patients compared with controls,
41 suggesting that 24B3 could be useful for early onset of AD diagnosis.

42

43 **Keywords:** Alzheimer's disease; amyloid β ; antibody; protein kinase C;

44 solid-phase peptide synthesis

45

46

47

48

49

50

51 **The opportunity to start this research**

52 First, I would like to explain the background to this study. My first original paper [1] was
53 on the isolation and Epstein–Barr virus-inducing activity of (–)-indolactam-V (IL-V) [2],
54 the basic ring structure of teleocidins [3-5], from *Streptomyces blastmyceticum*. IL-V is a
55 tumor promoter and activator of protein kinase C (PKC) isozymes [6,7], the key enzyme
56 family involved in signal transduction on the cell surface [8]. Since *Streptomyces*
57 *blastmyceticum* produces a large amount of IL-V, detailed structure–activity relationship
58 studies were performed to clarify the structural requirements of its tumor-promoting
59 activity [9,10]. Consequently, the next step was to identify the binding mode of IL-V with
60 PKC isozymes, whose binding sites are two C1 domains: C1A and C1B [11-13]. For this
61 purpose, it was necessary to prepare PKC isozymes in sufficient quantity. However, there
62 were difficulties in obtaining PKC isozymes with potent binding affinity to various PKC
63 ligands; namely, phorbol 12,13-dibutyrate (PDBu), IL-V, and teleocidins. Specifically,
64 the C1 domains were highly sensitive to oxidation because of their cysteine-rich sequence
65 with a zinc-finger-like structure (ring-finger).

66 In 1992, I was in Stanford University as a visiting scholar, when Professor Paul A.
67 Wender advised me to synthesize each PKC C1 domain by solid-phase peptide synthesis.
68 Based on his advice, two PKC γ C1 domain peptides (PKC γ -C1A and PKC γ -C1B) of
69 approximately 50 amino acid residues were custom synthesized at Stanford University.
70 Fortunately, we detected weak but significant [3 H]PDBu binding against each of them,
71 although their purity and binding constants (K_d) were not satisfactory [14]. After returning
72 home in 1993, I started to establish a synthetic method of long peptides without fragment
73 condensation in collaboration with Dr. Hiroyuki Fukuda at Applied Biosystems, Japan.
74 After struggling for five years, we eventually succeeded in synthesizing all PKC isozyme
75 C1 domains at high purity, and were able to precisely determine their K_d values against

76 [3H]PDBu [15-17]. The representative example (PKC δ -C1B) is shown in Figure 1. This
77 data provided the basis for rational design of new medicinal leads with PKC isozyme
78 selectivity. Moreover, we identified diacylglycerol kinase (DGK) β and γ as new PDBu
79 receptors using synthetic C1 peptides of all DGK isozymes [18]. We were even able to
80 synthesize a 116-mer PKC γ -C1A-C1B peptide without fragment condensation [19]. The
81 core method of this synthesis consists of three points: polyethylene glycol polystyrene
82 support as a resin, hexafluorophosphate azabenzotriazole tetramethyl uronium (HATU)
83 developed by Carpino [20] as a highly efficient activator, and the continuous flow-type
84 peptide synthesizer, PioneerTM supplied by Applied Biosystems. Unfortunately, this
85 machine has been out of service since 2008, and we have recently introduced a
86 microwave-type peptide synthesizer, Biotage Initiator+ AlstraTM (Biotage). The
87 opportunity to start my research was the establishment of this peptide synthesis
88 technology, and also my encounter with Dr. Fukuda, who collaborated with Dr. Takuji
89 Shirasawa at Tokyo Metropolitan Institute of Gerontology, a world-renowned scientist in
90 amyloid β research.

91

92 **Toxic conformation theory of amyloid β**

93 Alzheimer's disease (AD) is one of the most common neurodegenerative disorders,
94 characterized by extracellular amyloid fibrils and intracellular neurofibrillary tangles
95 (Figure 2) [21]. The former consist mainly of 40- or 42-mer amyloid β protein (A β 40 and
96 A β 42), while the latter are composed of hyperphosphorylated tau protein. AD proceeds
97 along a sequence of aggregation (oligomerization) of A β , hyperphosphorylation of tau
98 protein, and ultimately, loss of nerve cells (amyloid hypothesis, Figure 3) [22]. More
99 recently, accumulated evidence suggests that soluble A β oligomers, rather than A β fibrils,
100 play a more important role in the pathogenesis of AD because of their more potent

101 neurotoxicity [23-25]. In 1999, when I began my research on A β , the molecular
102 mechanism of A β aggregation and neurotoxicity had not been determined, and even the
103 secondary structure of the “toxic oligomers” remained unknown. The main reasons for
104 this were because of difficulties in the synthesis of A β 42, the most toxic and highly
105 aggregative species, and its highly aggregative character, making high-resolution X-ray
106 crystallography and liquid-phase nuclear magnetic resonance (NMR) analysis almost
107 impossible. Although solid-phase NMR analysis on aggregates of A β 40, the less
108 neurotoxic and less aggregative species, were first reported by Tycko’s group in 2002
109 [26], there were few reports on the precise structure of A β 42 aggregates until 2015 [27-
110 29].

111 First, a systematic proline replacement approach was adopted to identify the
112 secondary structure of A β 42 responsible for its potent aggregative ability and
113 neurotoxicity. Prolines are not present in β -sheet structures but are easily accommodated
114 in turn structures. Wood *et al.*, [30] reported the first proline replacement on A β
115 fragments (A β 15–23 and A β 12–26), and suggested that the residues at position 17–23
116 are involved in intermolecular β -sheets of A β fibrils. However, such replacements should
117 be performed using full-length A β 42, whose solid-phase synthesis is difficult because of
118 its last 14 C-terminal hydrophobic and bulky amino acid residues. As described, my
119 colleagues and I had developed a practical and efficient method to synthesize
120 hydrophobic and bulky peptides of over 50 amino acid residues without fragment
121 condensation [15], enabling the flexible replacement of each amino acid residue of A β 42
122 with proline [31,32].

123 Approximately 40 proline-substituted mutants of A β 42 were synthesized to examine
124 their aggregative velocity, thermodynamic stability of their aggregates, and neurotoxicity
125 against rat pheochromocytoma (PC12) cells. The resultant data suggested that the

126 residues at positions 15–21 and 24–32 were involved in the intermolecular β -sheet
 127 structure of A β 42 aggregates, and that the turn at position 22 and 23 plays a critical role
 128 in aggregation and neurotoxicity of A β 42. Notably, mutation sites in familial AD are
 129 concentrated at this position [33,34]. Although the N-terminal 13 residues did not adopt
 130 any solid structure in A β 42 aggregates, the C-terminal eight residues participated in their
 131 intramolecular β -sheet structure [35]. Based on these findings, we proposed toxic dimer
 132 and trimer models, as shown in Figure 4 [36].

133 Several reports suggested that radicalization of both Tyr10 and Met35 was important
 134 for inducing aggregation and neurotoxicity of A β 42 [37–39]. Radicalization of Tyr10 by
 135 coordinated Cu(II) at His residues at positions 6, 13, and 14 of A β 42 is considered to be
 136 an initial event for A β 42 to aggregate and induce neurotoxicity [40]. Accordingly, Tyr10
 137 could be converted to a phenoxy radical by the reaction of Cu(II) to Cu(I) to obtain
 138 hydrogen peroxide. In our model, phenoxy radical can efficiently oxidize Met35 by
 139 formation of a turn at position 22 and 23, bringing Tyr10 and Met35 closer together
 140 [41,42]. The resultant cation radical of Met35 can be ionically stabilized by the C-
 141 terminal carboxylate of Ala42, forming a hydrophobic core that accelerates aggregation
 142 to form a dimer and trimer. Since carboxyl radicals are incorporated in aggregates,
 143 liberation of these radicals will cause oxidative stress against neuronal cells for extended
 144 periods of time. This is our “toxic conformation theory”, and the turn at position 22 and
 145 23 is called a “toxic turn” (Figure 4).

146 To confirm the presence of the toxic turn, solid-state NMR of partially ^{13}C - and ^{15}N -
 147 labeled A β 42 at positions 21–24 or 25–27 was measured after aggregation using ^{13}C -1H
 148 dipolar assisted rotational resonance [43,44], in collaboration with Professor Kiyonori
 149 Takegoshi at Kyoto University. The data clearly showed the presence of turns at position
 150 22 and 23 and position 25 and 26 in aggregates of wild-type A β 42 and E22K-A β 42

151 (Italian mutation for familial AD [45]) [46,47]. Moreover, conformationally-fixed A β 42
152 with a lactam ring at position 22 and 23 was neurotoxic, while a lactam ring at position
153 25 and 26 was virtually non-toxic [47]. A β 42 is produced from amyloid precursor protein
154 (APP) by two secretases [48]. A β 42 monomer is in equilibrium between two conformers
155 with a turn at positions 22 and 23 or 25 and 26, with the former aggregating to form toxic
156 oligomers (Figure 5).

157 Systematic proline replacement of A β 40 was also reported by Wetzel's group in
158 2004 [49]. Although the C-terminal structure of A β 40 is different from A β 42, the turn at
159 position 22 and 23 was also present in A β 40 aggregates. The turn mimic peptide, E22P-
160 A β 40, was more aggregative and neurotoxic compared with wild-type A β 40, suggesting
161 that the turn at position 22 and 23 in A β 40 was pathological [31,32]. However, the
162 position of the turn determined by solid-state NMR was different in A β 40 aggregates [26]
163 (Figure 6). The turn was present near position 25 and 26, which is similar to the nontoxic
164 conformer in A β 42 aggregates [47], because of the presence of a salt bridge between
165 Asp23 and Lys28.

166 Recently, the structure of highly homogeneous A β 42 aggregates determined by
167 solid-state NMR was independently reported by three groups [27-29]. Surprisingly, the
168 turn position in A β 42 aggregates was quite different from that in A β 40 aggregates: in the
169 former, it was near position 22 and 23, while it was near position 25 and 26 in the latter.
170 Both of these positions correlate with our proposed turn structures in A β 42 aggregates
171 (Figure 6). The presence of Ile41 and Ala42 at the C-terminus of A β 42 could create a salt
172 bridge between the primary ammonium ion of Lys28 and carboxylate anion of Ala42 to
173 fix the molecule with a turn at position 22 and 23, unlike A β 40. This clearly demonstrates

174 that A β 42 is more aggregative and neurotoxic than A β 40 since the turn at position 22 and
175 23 is important to induce aggregation and neurotoxicity of A β .

176

177 **Synthesis and characterization of dimer models of A β**

178 As described, my colleagues and I identified the key structure (toxic turn) of A β 42 that
179 induces aggregation and neurotoxicity. Recent investigations suggest that A β oligomers
180 are more neurotoxic than mature A β fibrils [23-25]. However, A β oligomers are labile
181 and in complex equilibrium among monomers, several oligomers, and mature fibrils
182 (Figure 7). For example, 12-mers and 24-mers might form from dimers and/or trimers as
183 a minimum unit. Further, some A β oligomers are unable to form amyloid fibrils to exist
184 as quasi-stable oligomers (off-pathway), while others directly aggregate into fibrils (on-
185 pathway). It is difficult to separate pure oligomeric species for biological evaluation. To
186 solve this problem, two approaches have been attempted: stabilization of A β oligomers
187 by photo-induced cross-linking, and synthesis of chemically pure and stable A β oligomer
188 models.

189 Teplov's group isolated dimers, trimers, and tetramers of A β 40 using photo-induced
190 cross-linking after incubation, and showed that their neurotoxicity was higher than A β 40
191 monomers [50]. However, each oligomeric species might be a complex mixture of
192 compounds with different three-dimensional structures since various positions of cross-
193 linking are possible. It is therefore difficult to determine which three-dimensional
194 structure is responsible for the toxicity observed in neuronal cells. Alternatively, there are
195 several reports on the synthesis of dimer models of A β 40 [51-55]. Nonetheless, in all
196 cases, toxic conformation of A β 40 was not considered. Moreover, the linker positions
197 were almost within N-terminal regions rather than C-terminal ones which are involved in

198 the formation of a hydrophobic core to induce oligomerization (Figure 4). Most of these
 199 models formed aggregative amyloid fibrils, and some were neurotoxic [52,54,55].

200 Based on our toxic dimer model (Figure 4), three dimer models were synthesized:
 201 two with linkers at positions 30 or 38 of A β 40 (**1–3**), and one with a linker at position 40
 202 of A β 42 (**4**) [56,57] (Figure 8). L,L-2,6-Diaminopimelic acid (DAP) or L,L-2,6-
 203 diaminoazelaic acid (DAZ) were used as linkers. Although DAP was previously used by
 204 Kok *et al.*, [51] for the synthesis of a dimer model with a DAP linker at position 10 to
 205 mimic the dityrosine-linked dimer of A β 40, there have been no reports using DAZ as a
 206 linker for A β dimers. Since the distance between the two methyl groups of Ala30 in
 207 E22K-A β 42 aggregates was estimated by solid-state NMR to be 5–6 Å [58], the DAZ
 208 linker was preferable for simulating the intramolecular β -sheet at position 31–36 of the
 209 A β 40 dimer model. To mimic the toxic turn at position 22 and 23, the E22P-mutant was
 210 used.

211 Synthesis of **1–4** was started by preparation of optically pure di-Fmoc-L,L-DAP and
 212 di-Fmoc-L,L-DAZ. The method of Paradisi *et al.*, [59] was adopted, albeit with slight
 213 modifications [56]. Solid-phase synthesis on a continuous flow-type peptide synthesizer
 214 (Pioneer™) was performed using di-Fmoc-L,L-DAP or di-Fmoc-L,L-DAZ (0.5
 215 equivalent with respect to the loading peptide to avoid formation of a monocoupled
 216 peptide), in accordance with Kok's study [51]. The purity of the dimers (**1–4**) was > 98%,
 217 as determined by high performance liquid chromatography (HPLC) analysis and
 218 electrospray ionization-quadrupole time-of-flight-mass spectrometry (ESI-qTOF-MS)
 219 measurements. Further, dimer yields were 5.6, 3.1, 11.6, and 6.0%, respectively [56,57].

220 Although dimer **2**, with a DAZ linker, had higher β -sheet content than **1** with a DAP
 221 linker as expected, the neurotoxicity of **2** as well as **1** against SH-SY5Y neuroblastoma
 222 cell lines was absent, even at 10 μ M [56]. In contrast, dimer **3**, with a DAP linker in the

223 C-terminal hydrophobic core at position 38, exhibited more potent neurotoxicity than the
 224 corresponding monomer, E22P-A β 40. All these dimer models exhibited weak thioflavin-
 225 T (Th-T) fluorescence after 48 h incubation, which reflected the amount of A β aggregates,
 226 suggesting they exist as quasi-stable oligomeric species even after 24–48 h incubation
 227 [56].

228 However, characterization of the A β oligomers responsible for AD pathogenesis has
 229 been controversial. Conventional techniques such as sodium dodecyl sulfate–
 230 polyacrylamide gel electrophoresis (SDS-PAGE) and size-exclusion chromatography
 231 (SEC) can be useful for this purpose, but SDS induces A β oligomerization [60].
 232 Additionally, SEC cannot accurately determine molecular weight since there are no ideal
 233 calibration proteins for A β . Recently, ion mobility-mass spectrometry (IM-MS)
 234 combined with ESI as a native ionization technique, has enabled separation of various A β
 235 oligomers to accurately determine their molecular weight without using organic solvents
 236 that disrupt noncovalent interactions within A β oligomers [61–63]. In fact, 2–12-mer
 237 aggregates of A β 40 and A β 42 have been assigned by IM-MS. However, larger oligomers
 238 could not be detected because of the high aggregative velocity of A β monomers.

239 In collaboration with Dr. Kenji Hirose and Mr. Taiji Kawase at Japan Waters Ltd.,
 240 IM-MS measurements of **1–3** were performed after 4 h incubations [56]. Similar spectra
 241 were obtained even after 24 h incubations. The representative two-dimensional heat maps
 242 with m/z domains and drift times are shown in Figure 9. Dimers **1** and **2**, with a DAP or
 243 DAZ linker at position 30, existed predominantly as hexamers in monomer conversion (n
 244 = 3), with oligomer distribution of 2–12-mer ($n = 1–6$). In contrast, dimer **3**, with a DAP
 245 linker at position 38, existed as 12–24-mers ($n = 6–12$). The fact that only **3** exhibited
 246 more potent neurotoxicity than E22P-A β 40 monomer, suggests that hydrophobic
 247 interaction of the C-terminal region of A β is indispensable for formation of larger toxic

248 oligomers, and that the oligomer size necessary to induce neurotoxicity is around 20-mer
 249 in monomer conversion.

250 According to our “toxic-conformation theory”, formation of the C-terminal
 251 hydrophobic core may be the initial event for A β 42 to induce oligomer formation and
 252 exhibit neurotoxicity through radicalization (Figure 4) [36]. Although the C-terminal
 253 hydrophobic core could not easily form in A β 40, a DAP linker at position 38 enabled
 254 A β 40 to form toxic oligomers such as A β 42. In fact, the corresponding A β 42 version of
 255 **3**, E22P,V40DAP-A β 42 dimer (**4**), also existed as a 12–24-mer in monomer conversion
 256 ($n = 6–12$) (unpublished results), and was significantly neurotoxic [57]. Dimers **3** and **4**
 257 may thus be one of the practical toxic dimer models of A β since they form quasi-stable
 258 protofibrillar aggregates with potent neurotoxicity, and consequently can be regarded as
 259 “off-pathway” aggregates.

260

261 **Synthesis and characterization of trimer models of A β**

262 A β oligomers originated from A β dimers may be involved in the pathogenesis of
 263 AD [64-66]. However, several investigations have suggested involvement of A β trimers,
 264 which show more potent synapse toxicity such as inhibition of long-term potentiation
 265 (LTP) than A β dimers or tetramers [67,68]. There were no reports on the synthesis and
 266 characterization of full-length A β trimer models, although trimer models of A β fragments
 267 were synthesized [69,70]. As my colleagues and I had experienced previously with
 268 systematic proline replacement [31,32], such models should be made for full-length A β .
 269 There are two possible trimer models: one consists of two intermolecular parallel β -sheets,
 270 with an additional A β monomer bound to the dimer model, while the other is a propeller-
 271 type model, as shown in Figure 4. Recently, this type of trimer was identified by solid-

272 state NMR in 150 kDa oligomers of A β 42 [71]. Since the propeller-type model is quite
 273 different from the dimer models with intermolecular parallel β -sheets, we attempted to
 274 mimic this trimer structure.

275 After molecular modeling studies, 1,3,5-phenyltris-L-alanine (PtA) was adopted as
 276 a trimer linker to reproduce a stable trimer structure (Figure 10A) [72]. Synthesis of tri-
 277 Fmoc-PtA was performed based on the approach of Ritzén *et al.* [73]. With asymmetric
 278 hydrogenation, Imamoto's Rh-(*S,S*)-QuinoxP [74] produced excellent results (> 98% ee,
 279 > 98% de). Three trimer models of E22P-A β 40 with the PtA linker at position 34, 36, or
 280 38 (**5–7**) were synthesized on a microwave peptide synthesizer (Initiator+ Alstra™,
 281 Biotage) using tri-Fmoc-PtA (0.33 equivalent was used to avoid formation of partially
 282 coupled PtA) (Figure 10B). Using C4 and C18 columns, trimer models with E22P
 283 mutation of A β 40 (**5–7**) were obtained at yields of 0.58, 1.1, and 0.45% after HPLC
 284 purification. Purity was checked by HPLC analysis and molecular formulae confirmed
 285 by ESI-qTOF-MS measurements [72]. Unexpectedly, continuous flow-type peptide
 286 synthesizer (Pioneer™) without heating and microwave irradiation did not produce these
 287 target molecules, possibly because the molecular motion might be strongly restricted by
 288 the trimer linker, thereby suppressing coupling reactions by steric hinderance at room
 289 temperature.

290 With the trimer models (**5–7**), neurotoxicity against SH-SY5Y cells was far less
 291 compared with dimer model **3** and E22P-A β 40 monomer [72]. Only **7**, with a PtA linker
 292 at position 38, exhibited significant but weak neurotoxicity compared with E22P-A β 40.
 293 IM-MS measurements suggested that an oligomer size of **7** was 9–21-mer in monomer
 294 conversion ($n = 3–7$), which is comparable to **3** (12–24-mer). In contrast, oligomer sizes
 295 of **5** and **6**, both without neurotoxicity, were 3–6-mer ($n = 1–2$) and 3–12-mer ($n = 1–4$),
 296 respectively. The 150 kDa oligomer of A β 42 [71] contained a trimer structure with an

297 anti-parallel β -sheet at the C-terminus. However, the corresponding trimer model **6** did
298 not exhibit any neurotoxicity, even at 10 μ M. In general, neurotoxicity of A β is
299 considered to be ascribable to the aggregation process, not specific oligomers [75]. Since
300 both **3** and **7** formed amyloid fibrils over 48 h incubation, this suggests that tertiary
301 structure as well as oligomer size can contribute to neurotoxicity. The concentration of
302 oligomers might also be important. Neurotoxicity (cell death) by aggregation at the cell
303 surface requires high oligomer concentration (>1 μ M), while synapse toxicity of
304 oligomers was observed at a low concentration (< 1 μ M) [24].

305 Hitherto, several correlations between oligomer size and neurotoxicity have been
306 reported [24]. For example, ADDL (3–24-mer) [76] and A β O (15–20-mer) [77] are
307 neurotoxic, while synapse toxicity such as LTP was induced by A β *56 (12-mer) [78] and
308 even a dimer or trimer of A β . This indicates that the oligomer size necessary for
309 neurotoxicity and synapse toxicity can be quite different. In addition, the presence of
310 larger oligomers, such as protofibrils (36–700-mer) [79] and amylospheroids (~ 150-mer)
311 [80], suggests that specific oligomers alone cannot explain neurotoxicity. Our data
312 suggests that at least A β oligomers < 12 -mer are not neurotoxic. Synapse toxicity of the
313 trimer models is thus worth investigating. However, caution should be applied since
314 synthetic oligomers do not always reflect the heterogeneous A β mixture present *in vivo*.

315

316 **Development of an anti-toxic-turn antibody, 24B3, and its application towards AD** 317 **diagnosis**

318 To identify the molecular species of A β oligomers that show neurotoxicity, it is
319 necessary to extract and purify applicable A β oligomers from human brain or
320 cerebrospinal fluid (CSF). However, structure–function analysis of A β oligomers is
321 problematic because A β oligomers are in complex equilibrium among monomers,

322 oligomers, and fibrils. To address this problem, anti-A β oligomer antibodies that
323 recognize the specific tertiary structure of each oligomer would be useful. Several anti-
324 A β oligomer antibodies have been developed, and some are widely used for A β research.
325 For example, A11 polyclonal antibody reacts with toxic oligomers of A β 42 more strongly
326 than its fibrillar aggregates [81]. Attention has also been given to NU1 as an A β oligomer-
327 specific antibody [82]. Moreover, anti-oligomeric (anti-protofibrillar) A β antibody
328 (BAN2401) has been developed for the treatment of AD [83]. The weak point of these
329 antibodies is that their epitopes are not clarified, and thus their usage in oligomer analyses
330 has several limitations.

331 My colleagues and I focused on the toxic turn of A β 42 at position 22 and 23, which
332 could be mimicked by proline substitution. At first, we obtained 11A1 antibody by
333 immunization to mice with E22P-A β 10-35 bound to a carrier protein [84]. 11A1 antibody
334 reacted not only with extracellular A β aggregates (senile plaques) but also with
335 intracellular A β aggregates, some of which were considered to be toxic oligomers.
336 Notably, intracellular A β oligomers were clearly detected in neurons differentiated from
337 induced pluripotent stem cells of AD patients [85]. However, reactivity of 11A1 against
338 senile plaques and monomeric A β was also high, making it difficult to use this antibody
339 as a diagnostic tool for AD.

340 Next, we focused on 24B3 antibody [57], which was obtained along with 11A1 by
341 screening using E22P-A β 42. This reacted strongly with E22P-A β 42 and the dimer
342 models, **3** and **4**, but unlike 11A1, hardly bound to wild-type A β 42 [57]. It was notable
343 that preincubated wild-type A β 42 was recognized by 24B3, indicating that toxic
344 oligomers derived from wild-type A β 42 could also bind to 24B3. These results prompted
345 us to generate a sandwich enzyme-linked immunosorbent assay (ELISA) in collaboration

346 with Immuno-Biological Laboratories (IBL) Co., Ltd., for potential application in early
347 AD diagnosis, since formation of toxic A β oligomers is considered to be an initial event
348 of AD [23-25]. After several trials, 82E1 [86], which recognizes the N-terminal-end of
349 A β , was fixed to a solid-phase for capture, while 24B3 conjugated with horseradish
350 peroxidase for detection was used for quantification of toxic oligomers with a toxic A β
351 turn in human CSF. To prove the concept of the “toxic-conformer theory”, human CSF
352 was analyzed using this ELISA in collaboration with Professor Takahiko Tokuda at
353 Kyoto Prefectural University of Medicine [57]. As shown in Figure 11, the ratio of toxic
354 conformer to total A β 42 in AD/mild cognitive impairment (MCI) patients was
355 significantly higher compared with age-matched non-AD controls. Nonetheless, a
356 significant difference in the amount of toxic conformer between AD/MCI and control
357 groups was not observed, possibly because of the small number of samples. Indeed, Akiba
358 *et al.*, [87] reported significantly high levels of the toxic conformer in AD patients using
359 our ELISA kit. They also suggested that the ratio of toxic conformer to total A β 42 in
360 patients with idiopathic normal pressure hydrocephalus (iNPH) was significantly higher
361 than control groups. This indicates that the toxic conformer ratio could be a reliable
362 biomarker for predicting the likelihood of patients with iNPH progressing into AD.

363 The 24B3 and 11A1 antibodies significantly suppressed neurotoxicity induced by
364 A β 42 and E22P-A β 42, whereas 82E1 and 4G8 (sequence-specific antibodies against
365 region 18–23 of A β) [88] did not [57]. The protective effect of 24B3 was higher than
366 11A1. Based on these results, passive immunization of 24B3 against AD model mice
367 (Tg2576) was examined in collaboration with Dr. Takahiko Shimizu at Chiba University
368 [89]. Intraperitoneal administration for 3 months (10 mg/kg/week) improved cognitive
369 impairment, although the number of senile plaques did not change. Moreover, even single
370 intravenous administration (20 mg/kg) suppressed the memory deficit. Masking of toxic

371 oligomers by 24B3 could lead to effective AD therapies with little adverse effects if 24B3
372 was reproduced for human use.

373 To investigate the contribution of the toxic conformer with the toxic turn to AD
374 pathogenesis, in collaboration with Dr. Shimizu, we recently developed a new AD mouse
375 model with E22P-A β mutation using a knock-in technique to avoid the artificial
376 phenotype observed in transgenic-type model mice [90]. Interestingly, a trimer band and
377 high molecular-weight oligomer bands (but not a monomer band) were detected in a Tris
378 buffer-soluble fraction of E22P-A β knock-in mice at six months of age, when cognitive
379 impairment occurred in the novel object recognition test. These data suggest that the toxic
380 conformer of A β induced cognitive dysfunction mediated by toxic oligomer formation.
381 However, loss of neurons was not observed in these model mice, indicating that A β
382 oligomers induced only synapse toxicity such as inhibition of LTP without severe
383 neurotoxic effects. Onset of AD might require accumulation of toxic A β oligomers,
384 followed by hyper-phosphorylation of tau proteins. Toxic oligomers might act as
385 mediators for tau phosphorylation to result in neuronal loss. In this context, E22P-A β
386 knock-in mice would be a useful model for evaluating oligomer-induced cognitive
387 impairment in AD. In addition, synapse toxicity of the trimer models (5–7) should also
388 be evaluated.

389

390 **Summary and future perspectives**

391 As described, the antibody 24B3 developed on the basis of the “toxic conformation
392 theory” could be a useful tool for early diagnosis of AD. The next step is to optimize this
393 antibody based on X-ray crystallographic analysis of the hapten peptide and its Fab
394 domain complex. Structural optimization of the toxic dimer and trimer models for second
395 generation antibodies against toxic oligomers of A β is also a pressing need. Recently,

396 attention has been given to AD diagnosis using human plasma samples instead of CSF,
397 which is more invasive. Yanagisawa and colleagues proposed new analytical methods to
398 quantify the amount of A β peptides in plasma samples using mass spectrometry to predict
399 accumulation of A β in the brain [91]. Our own approach is to use a Simoa™ (single
400 molecule array) technology. Using this technology, Tokuda and colleagues established
401 the method to quantify the amount of phosphorylated-tau (p-tau) in human plasma, and
402 showed that p-tau levels were significantly higher in AD patients than non-AD controls
403 [92]. In collaboration with Professor Tokuda and Professor Juan C. Troncoso at the Johns
404 Hopkins University School of Medicine, we are measuring the amount of toxic conformer
405 in human plasma samples using Simoa™ technology (unpublished results).

406 Prevention and treatment of AD are indispensable after diagnosis of early onset. It
407 has been reported that many natural products (mainly flavonoids) suppress aggregation
408 and neurotoxicity of A β 42 [93,94]. However, their mechanism of action remains
409 unknown. Recently, we proposed three structural features required for suppression of
410 A β 42 aggregation [95]. These features are: a catechol moiety that reacts with Lys residues
411 of A β 42 after oxidation [96], planarity due to α,β -unsaturated carbonyl groups that ensure
412 intercalation of the molecule into the intermolecular β -sheet region in A β aggregates
413 [97,98], and carboxy groups of triterpenoids or anthraquinoids that form salt bridges with
414 Lys16 of A β 42 oligomers [99,100]. These structural features would be useful for
415 predicting new anti-A β 42 aggregative compounds from natural sources, which might
416 become promising lead compounds for protection against early onset of AD.

417 Treatment of AD is also a pressing need. Immunotherapy using anti-A β antibodies
418 has been extensively investigated [101,102] after pioneering work by Schenk and
419 colleagues in 1999 [103]. However, most attempts gave disappointing results. Possible
420 reasons for this might be that the antibodies used were not optimized for toxic species of

421 A β aggregates, and that administration time of the antibodies to AD patients was too late.
422 Although application of our 24B3 antibody [57] might be promising, considerable money
423 is required for drug development and antibody therapy. In addition, γ -secretase and β -
424 secretase inhibitors have also failed in clinical trials [104].

425 Another therapeutic approach has been performed using PKC activators. Cumulative
426 evidence suggests that inhibition of PKC α decreases the amount of A β ₄₂ and A β ₄₀, and
427 that activation of PKC ϵ enhances degradation of A β through endothelin converting
428 enzyme [105-107]. Bryostatin 1, isolated from bryozoan [108], is one of the most
429 promising PKC activators because of its low adverse effects such as tumor promotion and
430 proinflammatory activity [107,109]. However, low availability from natural sources and
431 structural complexity has hampered the supply for medicinal leads. To overcome these
432 issues, synthesis of simplified analogs of bryostatin 1 that potently activate PKC
433 [110,111], and practical synthetic methods of bryostatin 1 have been reported [112,113].
434 Our own approach was to develop new medicinal leads from naturally occurring PKC
435 ligands, phorbol esters, ingenol esters, teleocidins, and aplysiatoxins [114]. After
436 extensive structure–activity studies, aplysiatoxins were found to be the most promising
437 leads [115] since their hydrophobicity is relatively low, and their structure is regarded as
438 a conformationally-fixed analogue of diacylglycerol, an endogenous ligand for PKC
439 isozymes. Moreover, we have developed 10-Me-Aplog-1 [116], a simplified analogue of
440 aplysiatoxin isolated from sea hare [117], as a new PKC activator without tumor-
441 promoting and proinflammatory activities (Figure 12). Since 10-Me-Aplog-1 did not
442 show any tumor-promoting and proinflammatory activities, it might be effective for
443 decreasing toxic oligomers of A β .

444 I felt something like my destiny when I began to synthesize a simplified analogue of
445 aplysiatoxin as a surrogate of bryostatin 1 with Dr. Yu Nakagawa in 2007. My research

446 on the chemistry and biology of A β originated from the structural study of PKC C1
447 domains through peptide synthesis. Additionally, research on the treatment of AD
448 connected again with research on naturally occurring PKC ligands. That is why research
449 is interesting generally.

450

451 **Acknowledgements**

452 I would like to express many thanks to the staff and graduate students who worked
453 with me in the laboratory of Organic Chemistry in Life Sciences, Division of Food
454 Science & Biotechnology, Graduate School of Agriculture, Kyoto University, and to all
455 the collaborators in this study, most of them mentioned in the text and shown in the
456 references.

457 I would like to express my sincere thanks to Dr. Koichi Koshimizu, emeritus
458 professor of Kyoto University, for giving me the opportunity to study teleocidins, which
459 was the starting point for this study. At the beginning of this study, Dr. Hideo Hayashi,
460 emeritus professor of Osaka Prefectural University, provided much help and
461 encouragement. I would also like to thank Dr. Hajime Ohigashi, emeritus professor of
462 Kyoto University, for continuous support of my research. Finally, I would like to thank
463 the Japan Society for Bioscience, Biotechnology, and Agrochemistry (JSBBA) for
464 awarding me the JSBBA Award 2019.

465 I thank Rachel James, Ph.D., from Edanz Group (www.edanzediting.com/ac) for
466 editing a draft of this manuscript.

467

468 **Disclosure statement**

469 No potential conflict of interest was reported by the author.

470

471 **Funding**

472 This work was supported in part by Grants-in-Aid for Scientific Research (S)
473 (26221202), (A) (19H00921, 21258015, 18208011), (B) (16380080, 13460048), (C)
474 (11660109), Scientific Research on Innovative Areas “Frontier Research on Chemical
475 Communications (17H06405), and “Chemical Biology of Natural Products” (23102011)
476 from JSPS. This work was also supported in part by funds from The Uehara Memorial
477 Foundation, The Naito Science & Engineering Foundation, The Takeda Science
478 Foundation, and Asahi Group Foundation.

479

480

481

482

483

484

485

486

487

488

489

490

491

492

493

494

495

496 **References**

- 497 [1] Irie K, Hirota M, Hagiwara N, et al. The Epstein-Barr virus early antigen-inducing
498 indole alkaloids, (–)-indolactam V and its related compounds, produced by
499 Actinomycetes. *Agric Biol Chem.* 1984;48:1269-1274.
- 500 [2] Endo Y, Shudo K, Okamoto T. Molecular requirements for epigenetic modulators.
501 Synthesis of active fragments of teleocidins and lynchbyatoxin. *Chem Pharm Bull.*
502 1982;30:3457-3460.
- 503 [3] Takashima M, Sakai H. A new toxic substance, teleocidin, produced by *Streptomyces*.
504 Part I. Production, isolation and chemical studies. *Bull Agr Chem Soc Jpn.*
505 1960;24:647-651.
- 506 [4] Nakata H, Harada H, Hirata Y. The structure of teleocidin B. *Tetrahedron Lett.*
507 1966;23:2515-2522.
- 508 [5] Hitotsuyanagi Y, Fujiki H, Suganuma M, et al. Isolation and structure elucidation of
509 teleocidin B-1, B-2, B-3 and B-4. *Chem Pharm Bull.* 1984;32:4233-4236.
- 510 [6] Fujiki H, Sugimura T. New class of tumor promoters: teleocidin, aplysiatoxin, and
511 palytoxin. *Adv Cancer Res.* 1987;49:223-264.
- 512 [7] Heikkilä J, Akerman KE. (–)-Indolactam V activates protein kinase C and induces
513 changes in muscarinic receptor functions in SH-SY5Y human neuroblastoma cells.
514 *Biochem Biophys Res Commun.* 1989;162:1207-1213.
- 515 [8] Nishizuka Y. Protein kinase C and lipid signaling for sustained cellular responses.
516 *FASEB J.* 1995;9:484-496.
- 517 [9] Irie K, Koshimizu K. Chemistry of indole alkaloid tumor promoter teleocidins.
518 *Comments Agric Food Chem.* 1993;3:1-25.

- 519 [10] Irie K. Chemical studies on tumor promoter teleocidins: structure-activity
520 relationship and photoaffinity labeling. *Nippon Nogeikagaku Kaishi*. 1994;68:1289-
521 1296.
- 522 [11] Ono Y, Fujii T, Igarashi K, et al. Phorbol ester binding to protein kinase C requires
523 a cysteine-rich zinc-finger-like sequence. *Proc Natl Acad Sci USA*. 1989;86:4868-
524 4871.
- 525 [12] Hurley JH, Newton AC, Parker PJ, et al. Taxonomy and functions of C1 protein
526 kinase C homology domains. *Protein Sci*. 1997;6:477-480.
- 527 [13] Zhang G, Kazanietz MG, Blumberg PM, et al. Crystal structure of the Cys2 activator-
528 binding domain of protein kinase C δ in complex with phorbol ester. *Cell*.
529 1995;81:917-924.
- 530 [14] Wender PA, Irie K, Miller BL. Identification, activity, and structural studies of
531 peptides incorporating the phorbol ester-binding domain of protein kinase C. *Proc*
532 *Natl Acad Sci USA*. 1995;92:239-243.
- 533 [15] Irie K, Oie K, Nakahara A, et al. Molecular basis for protein kinase C isozyme-
534 selective binding: the synthesis of the cysteine-rich domains of all protein kinase C
535 isozymes. *J Am Chem Soc*. 1998;120:9159-9167.
- 536 [16] Irie K, Nakahara A, Nakagawa Y, et al. Establishment of a binding assay for protein
537 kinase C isozymes using synthetic C1 peptides and development of new medicinal
538 leads with protein kinase C isozyme and C1 domain selectivity. *Pharm Ther*.
539 2002;93:271-281.
- 540 [17] Irie K, Nakagawa Y, Ohigashi H. Toward the development of new medicinal leads
541 with selectivity for protein kinase C isozymes. *Chem Rec*. 2005;5:185-195.
- 542 [18] Shindo M, Irie K, Masuda A, et al. Synthesis and phorbol ester binding of the
543 cysteine-rich domains of diacylglycerol kinase (DGK) isozymes. DGK γ and DGK β

- 544 are new targets of tumor-promoting phorbol esters. *J Biol Chem.* 2003;278:18448-
545 18454.
- 546 [19] Fukuda H, Irie K, Nakahara A, et al. Solid-phase synthesis, mass spectrometric
547 analysis of the zinc-folding, and phorbol ester-binding studies of the 116-mer peptide
548 containing the tandem cysteine-rich C1 domains of protein kinase C gamma. *Bioorg*
549 *Med Chem.* 1999;7:1213-1221.
- 550 [20] Carpino LA. 1-Hydroxy-7-azabenzotriazole. An efficient peptide coupling additive.
551 *J Am Chem Soc.* 1993;115:4397-4398.
- 552 [21] Haass C, Selkoe DJ. Soluble protein oligomers in neurodegeneration: lessons from
553 the Alzheimer's amyloid beta-peptide. *Nat Rev Mol Cell Biol.* 2007;8:101-112.
- 554 [22] Selkoe DJ, Hardy J. The amyloid hypothesis of Alzheimer's disease at 25 years.
555 *EMBO Mol Med.* 2016;8:595-608.
- 556 [23] Walsh DM, Klyubin I, Fadeeva JV, et al. Naturally secreted oligomers of amyloid β
557 protein potently inhibit hippocampal long-term potentiation in vivo. *Nature.*
558 2002;416:535-539.
- 559 [24] Benilova I, Karran E, De Strooper B. The toxic A β oligomer and Alzheimer's
560 disease: an emperor in need of clothes. *Nat Neurosci.* 2012;15:349-357.
- 561 [25] Ono, K. Alzheimer's disease as oligomeropathy. *Neurochem Int.* 2018;119:57-70.
- 562 [26] Petkova AT, Ishii Y, Balbach JJ, et al. A structural model for Alzheimer's β -amyloid
563 fibrils based on experimental constraints from solid state NMR. *Proc Natl Acad Sci*
564 *USA.* 2002;99:16742-16747.
- 565 [27] Xiao Y, Ma B, McElheny D, et al. A β (1-42) fibril structure illuminates self-
566 recognition and replication of amyloid in Alzheimer's disease. *Nat Struct Mol Biol.*
567 2015;22:499-505.

- 568 [28] Colvin MT, Silvers R, Ni QZ, et al. Atomic resolution structure of monomorphic
569 A β 42 amyloid fibrils. *J Am Chem Soc.* 2016;138:9663-9674.
- 570 [29] Wälti MA, Ravotti F., Arai H, et al. Atomic-resolution structure of a disease-relevant
571 A β (1-42) amyloid fibril. *Proc Natl Acad Sci USA.* 2016;113:E4976-E4984.
- 572 [30] Wood SJ, Wetzel R, Martin JD, et al. Prolines and amyloidogenicity in fragments of
573 the Alzheimer's peptide β /A4. *Biochemistry.* 1995;34:724-730.
- 574 [31] Morimoto A, Irie K, Murakami K, et al. Aggregation and neurotoxicity of mutant
575 amyloid β (A β) peptides with proline replacement: importance of turn formation at
576 positions 22 and 23. *Biochem Biophys Res Commun.* 2002;295:306-311.
- 577 [32] Morimoto A, Irie K, Murakami K, et al. Analysis of the secondary structure of β -
578 amyloid (A β 42) fibrils by systematic proline replacement. *J Biol Chem.*
579 2004;279:52781-52788.
- 580 [33] Murakami K, Irie K, Morimoto A, et al. Neurotoxicity and physicochemical
581 properties of A β mutant peptides from cerebral amyloid angiopathy: implication for
582 the pathogenesis of cerebral amyloid angiopathy and Alzheimer's disease. *J Biol*
583 *Chem.* 2003;278:46179-46187.
- 584 [34] Izuo N, Kume T, Sato M, et al. Toxicity in rat primary neurons through the cellular
585 oxidative stress induced by the turn formation at positions 22 and 23 of A β 42. *ACS*
586 *Chem Neurosci.* 2012;3:674-681.
- 587 [35] Masuda Y, Uemura S, Nakanishi A, et al. Verification of the C-terminal
588 intramolecular β -sheet in A β 42 aggregates using solid-state NMR: implications for
589 potent neurotoxicity through the formation of radicals. *Bioorg Med Chem Lett.*
590 2008;18:3206-3210.

- 591 [36] Irie K, Murakami K, Masuda Y, et al. Structure of β -amyloid fibrils and its relevance
592 to their neurotoxicity: implications for the pathogenesis of Alzheimer's disease. *J*
593 *Biosci Bioeng.* 2005;99:437-447.
- 594 [37] Barnham KJ, Haeffner F, Ciccotosto GD, et al. Tyrosine gated electron transfer is
595 key to the toxic mechanism of Alzheimer's disease of β -amyloid. *FASEB J.*
596 2004;18:1427-1429.
- 597 [38] Varadarajan S, Yatin S, Kanski J, et al. Methionine residue 35 is important in amyloid
598 β -peptide-associated free radical oxidative stress. *Brain Res Bull.* 1999;50:133-141.
- 599 [39] Varadarajan S, Kanski J, Aksenova M, et al. Different mechanisms of oxidative
600 stress and neurotoxicity for Alzheimer's $A\beta(1-42)$ and $A\beta(25-35)$. *J Am Chem Soc.*
601 2001;123:5625-5631.
- 602 [40] Curtain CC, Ali F, Volitakis I, et al. Alzheimer's disease amyloid- β binds copper
603 and zinc to generate an allosterically ordered membrane-penetrating structure
604 containing superoxide dismutase-like subunits. *J Biol Chem.* 2001;276:20466-20473.
- 605 [41] Murakami K, Hara H, Masuda Y, et al. Distance measurement between Tyr10 and
606 Met35 in amyloid β by site-directed spin-labeling ESR spectroscopy: implications for
607 the stronger neurotoxicity of $A\beta_{42}$ than $A\beta_{40}$. *ChemBioChem.* 2007;8:2308-2314.
- 608 [42] Murakami K, Irie K, Ohigashi H, et al. Formation and stabilization model of the 42-
609 mer $A\beta$ radical: implications for the long-lasting oxidative stress in Alzheimer's
610 disease. *J Am Chem Soc.* 2005;127:15168-15174.
- 611 [43] Takegoshi K, Nakamura S, Terao T. ^{13}C - ^1H dipolar-assisted rotational resonance in
612 magic-angle spinning NMR. *Chem Phys Lett.* 2001;344:631-637.
- 613 [44] Takegoshi K, Nakamura S, Terao T. ^{13}C - ^1H dipolar driven ^{13}C - ^{13}C recoupling
614 without ^{13}C rf irradiation in nuclear magnetic resonance of rotating solids. *J Chem*
615 *Phys.* 2003;118:2325-2341.

- 616 [45] Miravalle L, Tokuda T, Chiarle R, et al. Substitutions at codon 22 of Alzheimer's A
617 peptide induce diverse conformational changes and apoptotic effects in human
618 cerebral endothelial cells. *J Biol Chem.* 2000;275: 27110-27116.
- 619 [46] Masuda Y, Irie K, Murakami K, et al. Verification of the turn at positions 22 and 23
620 of the beta-amyloid fibrils with Italian mutation using solid-state NMR. *Bioorg Med*
621 *Chem.* 2005;13:6803-6809.
- 622 [47] Masuda Y, Uemura S, Ohashi R, et al. Identification of physiological and toxic
623 conformations in A β 42 aggregates. *ChemBioChem.* 2009;10:287-295.
- 624 [48] De Strooper B. Proteases and proteolysis in Alzheimer's disease: a multifactorial
625 view on the disease process. *Physiol Rev.* 2010;90:465-494.
- 626 [49] Williams AD, Portelius E, Kheterpal I, et al. Mapping A β amyloid fibril secondary
627 structure using scanning proline mutagenesis. *J Mol Biol.* 2004;335:833-842.
- 628 [50] Ono K, Condrón MM, Teplow DB. Structure-neurotoxicity relationships of amyloid
629 β -protein oligomers. *Proc Natl Acad Sci USA* 2009;106:14745-14750.
- 630 [51] Kok WM, Scanlon DB, Karas JA, et al. Solid-phase synthesis of homodimeric
631 peptides: preparation of covalently-linked dimers of amyloid β peptides. *Chem*
632 *Commun.* 2009;6228-6230.
- 633 [52] O'Nuallain B, Freire DB, Nicoll AJ, et al. Amyloid β -protein dimers rapidly form
634 stable synaptotoxic protofibrils. *J Neurosci.* 2010;30:14411-14419.
- 635 [53] Yamaguchi T, Yagi H, Goto Y, et al. A disulfide-linked amyloid- β peptide dimer
636 forms a protofibril-like oligomer through a distinct pathway from amyloid fibril
637 formation. *Biochemistry.* 2010;49:7100-7107.
- 638 [54] Kok WM, Cottam JM, Ciccotosto GD, et al. Synthetic dityrosine-linked β -amyloid
639 dimers form stable, soluble, neurotoxic oligomers. *Chem Sci.* 2013;4:4449-4454.

- 640 [55] O'Malley TT, Oktaviani NA, Zhang D, et al. A β dimers differ from monomers in
641 structural propensity, aggregation paths and population of synaptotoxic assemblies.
642 *Biochem J.* 2014;461:413-426.
- 643 [56] Irie Y, Murakami K, Hanaki M, et al. Synthetic models of quasi-stable amyloid β 40
644 oligomers with significant neurotoxicity. *ACS Chem Neurosci.* 2017;8:807-816.
- 645 [57] Murakami K, Tokuda M, Suzuki T, et al. Monoclonal antibody with conformational
646 specificity for a toxic conformer of amyloid β 42 and its application toward the
647 Alzheimer's disease diagnosis. *Sci Rep.* 2016;6:29038.
- 648 [58] Masuda Y, Nakanishi A, Ohashi R, et al. Verification of the intermolecular parallel
649 β -sheet in E22K-A β 42 aggregates by solid-state NMR using rotational resonance:
650 implications for the supramolecular arrangement of the toxic conformer of A β 42.
651 *Biosci Biotechnol Biochem.* 2008;72:2170-2175.
- 652 [59] Paradisi F, Porzi G, Rinaldi S, et al. A simple asymmetric synthesis of (+)- and (-)-
653 2,6-diaminopimelic acids. *Tetrahedron: Asymmetry.* 2000;11:1259-1262.
- 654 [60] Watt AD, Perez KA, Rembach A, et al. Oligomers, fact or artefact? SDS-PAGE
655 induces dimerization of β -amyloid in human brain samples. *Acta Neuropathol.*
656 2013;125:549-564.
- 657 [61] Bernstein SL, Dupuis NF, Lazo ND, et al. Amyloid- β protein oligomerization and
658 the importance of tetramers and dodecamers in the aetiology of Alzheimer's disease.
659 *Nat Chem.* 2009;1:326-331.
- 660 [62] Klonecki M, Jablonowska A, Poznanski J, et al. Ion mobility separation coupled
661 with MS detects two structural states of Alzheimer's disease A β 1-40 peptide
662 oligomers. *J Mol Biol.* 2011;407:110-124.

- 663 [63] Österlund N, Moons R, Ilag LL, et al. Native ion mobility-mass spectrometry reveals
664 the formation of β -barrel shaped amyloid- β hexamers in a membrane-mimicking
665 environment. *J Am Chem Soc.* 2019;141:10440-10450.
- 666 [64] Klyubin I, Betts V, Wetzel AT, et al. Amyloid β protein dimer-containing human
667 CSF disrupts synaptic plasticity: prevention by systemic passive immunization. *J*
668 *Neurosci.* 2008;28:4231-4237.
- 669 [65] Shankar GM, Li S, Mehta TH, et al. Amyloid- β protein dimers isolated directly from
670 Alzheimer's brains impair synaptic plasticity and memory. *Nat Med.* 2008;14:837-
671 842.
- 672 [66] Lendel C, Bjerring M, Dubnovitsky A, et al. A hexameric peptide barrel as building
673 block of amyloid- β protofibrils. *Angew Chem Int Ed.* 2014;53:12756-12760.
- 674 [67] Townsend M, Shankar GM, Mehta T, et al. Effects of secreted oligomers of amyloid
675 β -protein on hippocampal synaptic plasticity: a potent role for trimers. *J Physiol.*
676 2006;572:477-492.
- 677 [68] Tomiyama T, Nagata T, Shimada H, et al. A new amyloid β variant favoring
678 oligomerization in Alzheimer's-type dementia. *Ann. Neurol.* 2008;63:377-387.
- 679 [69] Spencer RK, Li H, Nowick JS. X-ray crystallographic structures of trimers and
680 higher-order oligomeric assemblies of a peptide derived from A β (17-36). *J Am Chem*
681 *Soc.* 2014;136:5595-5598.
- 682 [70] Shinoda K, Sohma Y, Kanai M. Synthesis of chemically-tethered amyloid- β segment
683 trimer possessing amyloidogenic properties. *Bioorg Med Chem Lett.* 2015;25:2976-
684 2979.
- 685 [71] Huang D, Zimmerman MI, Martin PK, et al. Antiparallel β -sheet structure within the
686 C-terminal region of 42-residue Alzheimer's amyloid- β peptides when they form
687 150-kDa oligomers. *J Mol Biol* 2015;427:2319-2328.

- 688 [72] Irie Y, Hanaki M, Murakami K, et al. Synthesis and biochemical characterization of
689 quasi-stable trimer models of full-length amyloid β 40 with a toxic conformation.
690 Chem Commun. 2019;55:182-185.
- 691 [73] Ritzén A, Basu B, Wällberg A, et al. Phenyltrisalanine: a new, C_3 -symmetric,
692 trifunctional amino acid. Tetrahedron: Asymmetry. 1998:3491-3496.
- 693 [74] Imamoto T, Tamura K, Zhang Y, et al. Rigid P-chiral phosphine ligands with *tert*-
694 butylmethylphosphino groups for rhodium-catalyzed asymmetric hydrogenation of
695 functionalized alkenes. J Am Chem Soc. 2012;134:1754-1769.
- 696 [75] Wogulis M, Wright S, Cunningham D, et al. Nucleation-dependent polymerization
697 is an essential component of amyloid-mediated neuronal cell death. J Neurosci.
698 2005;25:1071-1080.
- 699 [76] Lambert MP, Barlow AK, Chromy BA, et al. Diffusible, nonfibrillar ligands derived
700 from $A\beta_{1-42}$ are potent central nervous system neurotoxins. Proc Natl Acad Sci USA.
701 1998;95:6448-6453.
- 702 [77] Deshpande A, Mina E, Glabe C, et al. Different conformations of amyloid β induce
703 neurotoxicity by distinct mechanisms in human cortical neurons. J Neurosci.
704 2006;26:6011-6018.
- 705 [78] Lesné S, Koh MT, Kotilinek L, et al. A specific amyloid- β protein assembly in the
706 brain impairs memory. Nature. 2006;440:352-357.
- 707 [79] Harper JD, Wong SS, Lieber CM, et al. Observation of metastable $A\beta$ amyloid
708 protofibrils by atomic force microscopy. Chem Biol. 1997;4:119-125.
- 709 [80] Noguchi A, Matsumura S, Dezawa M, et al. Isolation and characterization of patient-
710 derived, toxic, high mass amyloid β -protein ($A\beta$) assembly from Alzheimer's disease
711 brains. J Biol Chem. 2009;284:32895-32905.

- 712 [81] Kaye R, Head E, Thompson JL, et al. Common structure of soluble amyloid
713 oligomers implies common mechanism of pathogenesis. *Science* 2003;300:486-489.
- 714 [82] Lambert MP, Velasco PT, Chang L, et al. Monoclonal antibodies that target
715 pathological assemblies of A β . *J Neurochem.* 2007;100:23-35.
- 716 [83] Logovinsky V, Satlin A, Lai R, et al. Safety and tolerability of BAN2401 – a clinical
717 study in Alzheimer’s disease with a protofibril selective A β antibody. *Alzheimers Res*
718 *Ther.* 2018;8:14.
- 719 [84] Murakami K, Horikoshi-Sakuraba Y, Murata N, et al. Monoclonal antibody against
720 the turn of the 42-residue amyloid β -protein at positions 22 and 23. *ACS Chem*
721 *Neurosci.* 2010;1:747-756.
- 722 [85] Kondo T, Asai M, Tsukita K, et al. Modeling Alzheimer’s disease with iPSCs reveals
723 stress phenotypes associated with intracellular A β and differential drug
724 responsiveness. *Cell Stem Cell.* 2013;12:487-496.
- 725 [86] Horikoshi Y, Mori T, Maeda M, et al. A β N-terminal-end specific antibody reduced
726 β -amyloid in Alzheimer-model mice. *Biochem Biophys Res Commun.*
727 2004;325:384-387.
- 728 [87] Akiba C, Nakajima M, Miyajima M, et al. Change of amyloid- β 1-42 toxic
729 conformer ratio after cerebrospinal fluid diversion predicts long-term cognitive
730 outcome in patients with idiopathic normal pressure hydrocephalus. *J Alzheimers Dis.*
731 2018;63:989-1002.
- 732 [88] Hatami A, Monjazebe S, Glabe C. The anti-amyloid- β monoclonal antibody 4G8
733 recognizes a generic sequence-independent epitope associated with α -synuclein and
734 islet amyloid polypeptide amyloid fibrils. *J Alzheimers Dis.* 2016;50:517-525.
- 735 [89] Izuo N, Kasahara C, Murakami K, et al. A toxic conformer of A β 42 with a turn at
736 22-23 is a novel therapeutic target for Alzheimer’s disease. *Sci Rep.* 2017;7:11811.

- 737 [90] Izuo N, Murakami K, Fujihara Y, et al. An *App* knock-in mouse inducing the
738 formation of a toxic conformer of A β as a model for evaluating only oligomer-
739 induced cognitive decline in Alzheimer's disease. *Biochem Biophys Res Commun.*
740 2019;515:462-467.
- 741 [91] Nakamura A, Kaneko N, Villemagne V, et al. High performance plasma amyloid- β
742 biomarkers for Alzheimer's disease. *Nature.* 2018;554:249-254.
- 743 [92] Tatebe H, Kasai T, Ohmichi T, et al. Quantification of plasma phosphorylated tau to
744 use as a biomarker for brain Alzheimer pathology: pilot case-control studies including
745 patients with Alzheimer's disease and down syndrome. *Mol Neurodegener.*
746 2017;12:63.
- 747 [93] Williams RJ, Spencer JP. Flavonoids, cognition, and dementia: actions, mechanisms,
748 and potential therapeutic utility for Alzheimer disease. *Free Radic Biol Med.*
749 2012;52:35-45.
- 750 [94] Williams P, Sorribas A, Howes MJ. Natural products as a source of Alzheimer's
751 drug leads. *Nat Prod Rep.* 2011;28:48-77.
- 752 [95] Murakami K, Irie K. Three structural features of functional food components and
753 herbal medicine with amyloid β 42 anti-aggregation properties. *Molecules*
754 2019;24:E2125.
- 755 [96] Sato M, Murakami K, Uno M, et al. Site-specific inhibitory mechanism for amyloid
756 β 42 aggregation by catechol-type flavonoids targeting the Lys residues. *J Biol Chem.*
757 2013;288:23212-23224.
- 758 [97] Hanaki M, Murakami K, Akagi K, et al. Structural insights into mechanisms for
759 inhibiting amyloid β 42 aggregation by non-catechol-type flavonoids. *Bioorg Med*
760 *Chem.* 2016;24:304-313.

- 761 [98] Hanaki M, Murakami K, Katayama S, et al. Mechanistic analyses of the suppression
762 of amyloid β 42 aggregation by apomorphine. *Bioorg Med Chem.* 2018;26:1538-
763 1546.
- 764 [99] Yoshioka T, Murakami K, Ido K, et al. Semisynthesis and structure-activity studies
765 of uncarinic acid C isolated from *Uncaria rhynchophylla* as a specific inhibitor of the
766 nucleation phase in amyloid β 42 aggregation. *J Nat Prod.* 2016;79:2521-2529.
- 767 [100] Murakami K, Yoshioka T, Horii S, et al. Role of the carboxy groups of triterpenoids
768 in their inhibition of the nucleation of amyloid β 42 required for forming toxic
769 oligomers. *Chem Commun.* 2018;54:6272-6275.
- 770 [101] van Dyck CH. Anti-amyloid- β monoclonal antibodies for Alzheimer's disease:
771 pitfalls and promise. *Biol Psychiatry.* 2018;83:311-319.
- 772 [102] Panza F, Lozupone M, Logroscino G, et al. A critical appraisal of amyloid- β -
773 targeting therapies for Alzheimer disease. *Nat Rev Neurol.* 2019;15:73-88.
- 774 [103] Schenk D, Barbour R, Dunn W, et al. Immunization with amyloid- β attenuates
775 Alzheimer-disease-like pathology in the PDAPP mouse. *Nature.* 1999;400:173-177.
- 776 [104] Panza F, Lozupone M, Dibello V, et al. Are antibodies directed against amyloid- β
777 ($A\beta$) oligomers the last call for the $A\beta$ hypothesis of Alzheimer's disease?
778 *Immunother.* 2019;11:3-6.
- 779 [105] Choi DS, Wang D, Yu GQ, et al. PKC ϵ increases endothelin converting enzyme
780 activity and reduces amyloid plaque pathology in transgenic mice. *Proc Natl Acad*
781 *Sci USA.* 2006;103:8215-8220.
- 782 [106] Khan TK, Nelson TJ, Verma VA, et al. A cellular model of Alzheimer's disease
783 therapeutic efficacy: PKC activation reverses $A\beta$ -induced biomarker abnormality on
784 cultured fibroblasts. *Neurobiol Dis.* 2009;34:332-339.

- 785 [107] Nelson TJ, Alkon DL. Neuroprotective versus tumorigenic protein kinase C
786 activators. *Trends Biochem Sci.* 2009;34:136-145.
- 787 [108] Pettit GR, Herald CL, Doubek DL, et al. Isolation and structure of bryostatin 1. *J*
788 *Am Chem Soc.* 1982;104:6846-6848.
- 789 [109] Halford B. The bryostatins' tale. *C&EN.* 2011;89(43):10-17.
- 790 [110] Wender PA, Baryza JL, Bennett CE, et al. The practical synthesis of a novel and
791 highly potent analogue of bryostatin. *J Am Chem Soc.* 2002;124:13648-13649.
- 792 [111] Keck GE, Kraft MB, Truong AP, et al. Convergent assembly of highly potent
793 analogues of bryostatin 1 via pyran annulation: bryostatin look-alikes that mimic
794 phorbol ester function. *J Am Chem Soc.* 2008;130:6660-6661.
- 795 [112] Trost BM, Dong G. Total synthesis of bryostatin 16 using atom-economical and
796 chemoselective approaches. *Nature.* 2008;456:485-488.
- 797 [113] Wender PA, Hardman CT, Ho S, et al. Scalable synthesis of bryostatin 1 and
798 analogs, adjuvant leads against latent HIV. *Science.* 2017;358:218-223.
- 799 [114] Irie K, Yanagita RC. Synthesis and biological activities of simplified analogs of the
800 natural PKC ligands, bryostatin-1 and aplysiatoxin. *Chem Rec.* 2014;14:251-267.
- 801 [115] Nakagawa Y, Yanagita RC, Hamada N, et al. A simple analogue of tumor-
802 promoting aplysiatoxin is an antineoplastic agent rather than a tumor promoter:
803 development of a synthetically accessible protein kinase C activator with bryostatin-
804 like activity. *J Am Chem Soc.* 2009;131:7573-7579.
- 805 [116] Kikumori M, Yanagita RC, Tokuda H, et al. Structure-activity studies on the
806 spiroketal moiety of a simplified analogue of debromoaplysiatoxin with
807 antiproliferative activity. *J Med Chem.* 2012;55:5614-5626.

808 [117] Kato Y, Scheuer PJ. Aplysiatoxin and debromoaplysiatoxin, constituents of the
809 marine mollusc *Stylocheilus longicauda* (Quoy and Gaimard, 1824). J Am Chem Soc
810 1974;96:2245-2246.

811

812

813

814

815

816

817

818

819

820

821

822

823

824

825

826

827

828

829

830

831

832

833 **Figure captions**

834 **Figure 1.** PKC δ -C1B domain peptide¹⁵⁾ and its crystal structure.¹³⁾

835 **Figure 2.** Senile plaques and neurofibrillary tangles in brain slices of AD patients, along
 836 with A β 42 and A β 40 sequences.

837 **Figure 3.** The amyloid hypothesis.²²⁾ MCI: mild cognitive impairment; AD: Alzheimer's
 838 disease.

839 **Figure 4.** Putative structure of dimers and trimers of A β 42 induced by radicalization.^{36,42)}
 840 Green arrows show intra- or intermolecular β -sheet regions in A β 42
 841 aggregates.

842 **Figure 5.** Toxic or less toxic conformers of A β 42.⁴⁷⁾

843 **Figure 6.** Structure of each monomer unit of aggregates of A β 42²⁷⁻²⁹⁾ and A β 40²⁶⁾
 844 revealed by solid-state NMR.

845 **Figure 7.** Putative structures of A β oligomers. It is not clear which oligomers are on-
 846 pathway, leading to amyloid fibrils, stable and less toxic species, and which
 847 oligomers are off-pathway, not resulting in fibril formation.

848 **Figure 8.** Structure of A β 40 dimer models with a linker at position 30 or 38 and A β 42
 849 dimer with a linker at position 40. The A β 40 dimer structure is based on
 850 proline scanning by Williams *et al.*⁴⁹⁾ Green arrows show intermolecular β -
 851 sheet regions in A β 40 aggregates.

852 **Figure 9.** Oligomer analysis of dimer and trimer models (**2**, **3**, **7**) by IM-MS after 4 h
 853 incubation at 12.5 μ M for **2** and **3**, and 8 μ M for **7** at 37 °C. *n* = number of
 854 dimers or trimers.

855 **Figure 10.** (A) Synthesis of (*S,S,S*)-tri-Fmoc-PtA. (a) 1,1,3,3-Tetramethyl guanidine,
 856 THF, 0 °C to room temperature, 4 h, 76%. (b) Rh-(*S,S*)-QuinoxP,⁷⁴⁾ H₂ (4
 857 atm), EtOAc/MeOH, room temperature, 4 h, 92% (>98%ee, >98%de). (c)

858 NaOHaq, MeOH, 1 h, 97%. (d) H₂, Pd/C, MeOH, overnight, 75%. (e) Fmoc-
859 OSu, Na₂CO₃, MeCN, H₂O, 3 d, 50%.

860 (B) Structure of trimer models (5–7) of E22P-Aβ40.

861 **Figure 11.** Sandwich ELISA of cerebrospinal fluid from AD patients.⁵⁷⁾

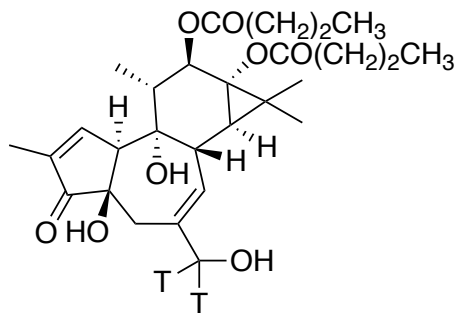
862 **Figure 12.** Structure of aplysiatoxin and its simplified analogue, 10-Me-Aplog-1.¹¹⁶⁾

863



H R F K V Y N Y M S P T F **C** D H **C** G S L L W G L V K Q G L K **C** E D **C** G M N V **H** H K **C** R E K V A N L **C** G

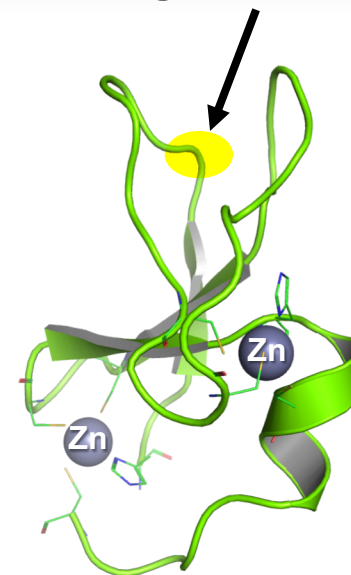
- 1) Solid-phase synthesis
- 2) Zinc-folding



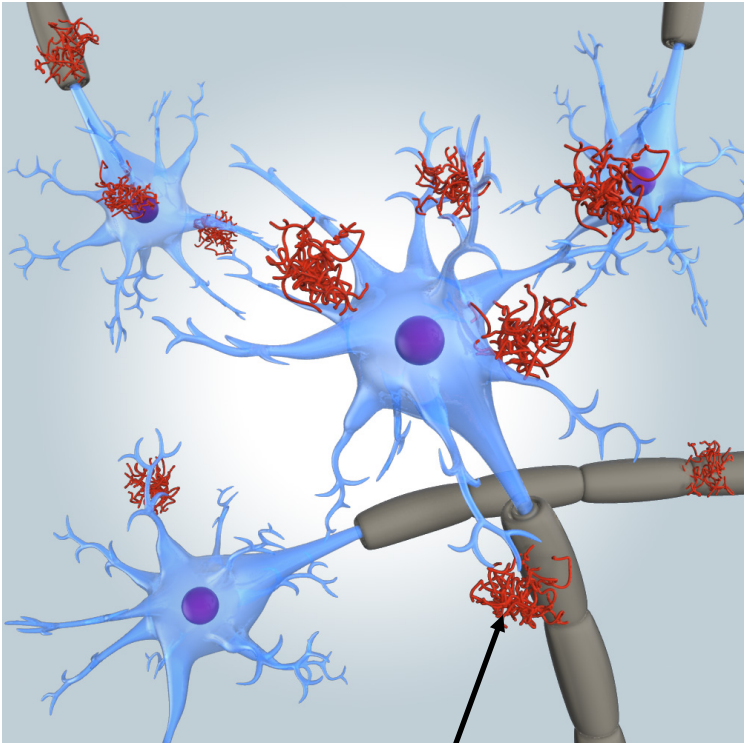
- 3) [3 H]PDBu binding assay

$$K_d = 0.53 \text{ nM}$$

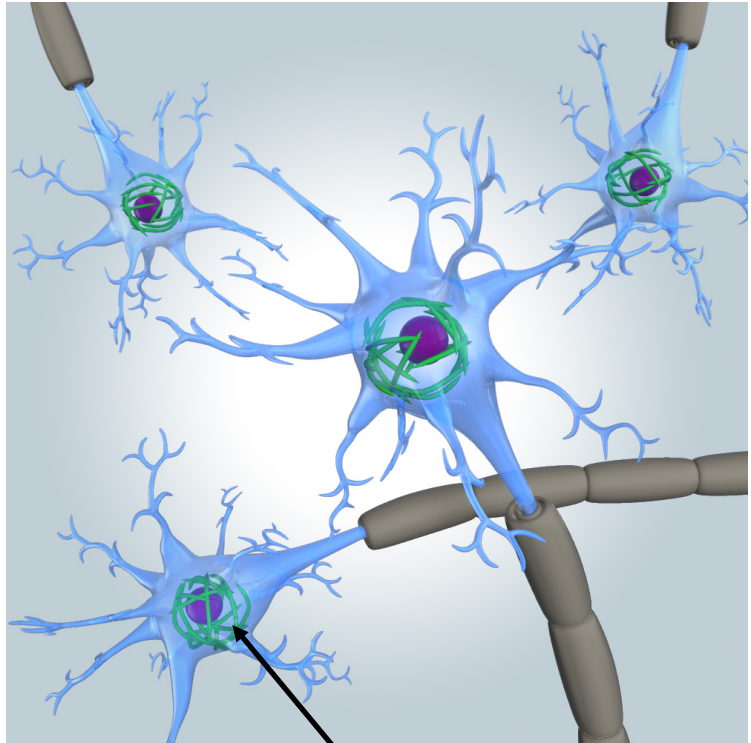
PKC ligand binding site



Crystal structure of δ -C1B



**Senile plaques
(A β aggregates)**



Neurofibrillary tangles

A β 42: DAEFRHDSGY EVHHQKLVFF AEDVGSNKGA IIGLMVGGVV IA
A β 40: DAEFRHDSGY EVHHQKLVFF AEDVGSNKGA IIGLMVGGVV

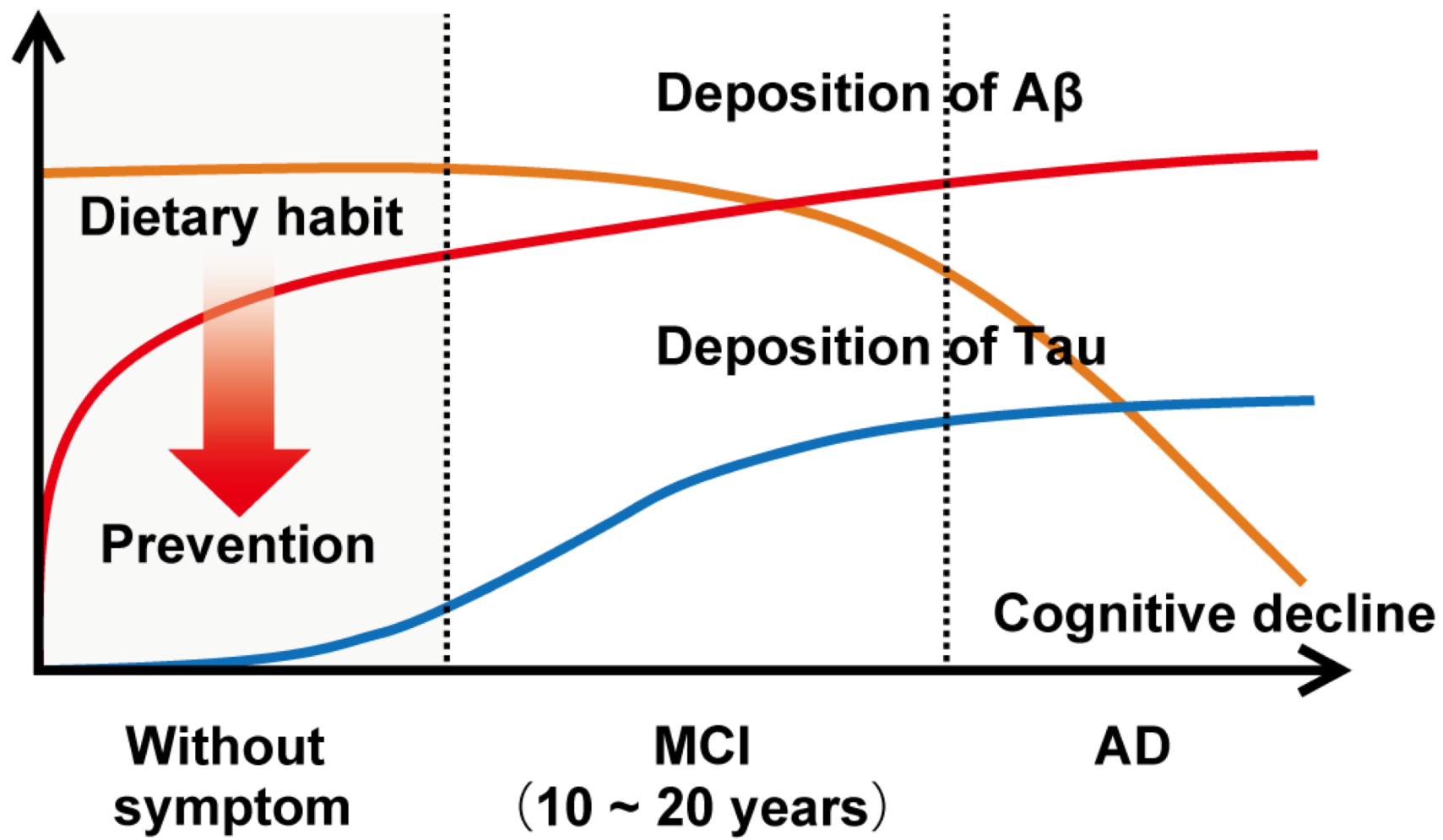


Figure 3

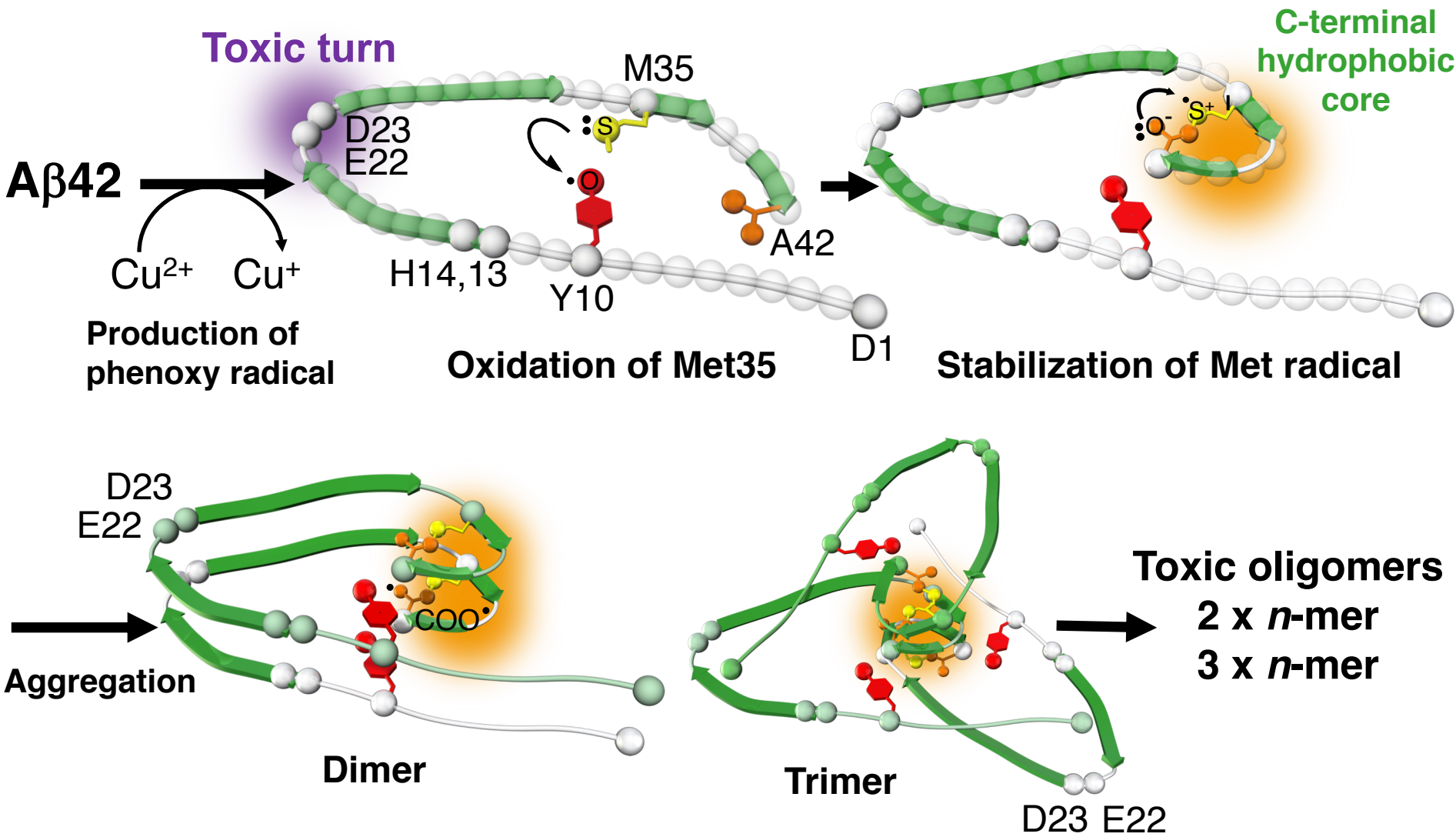


Figure 4

Amyloid precursor protein

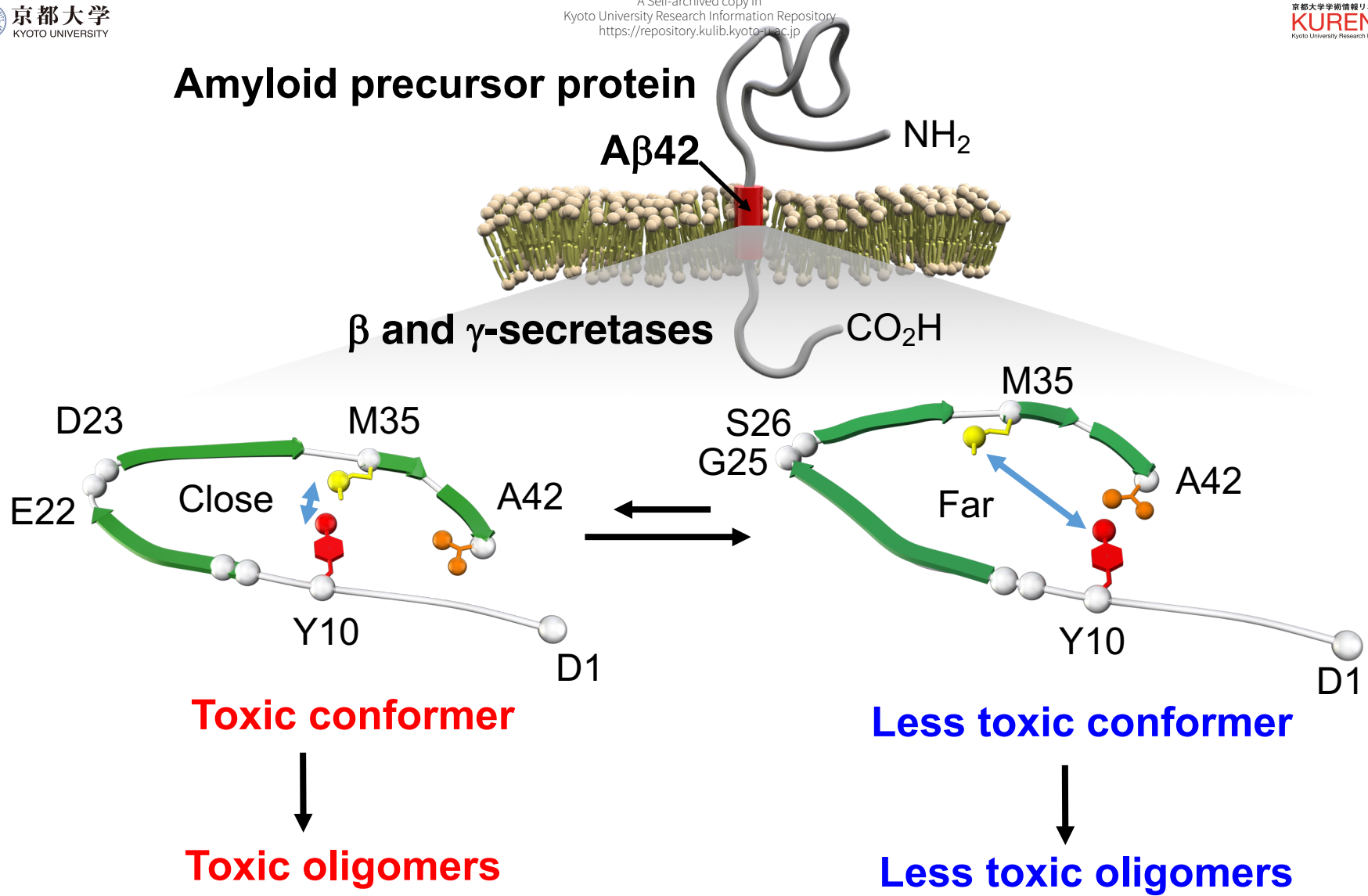
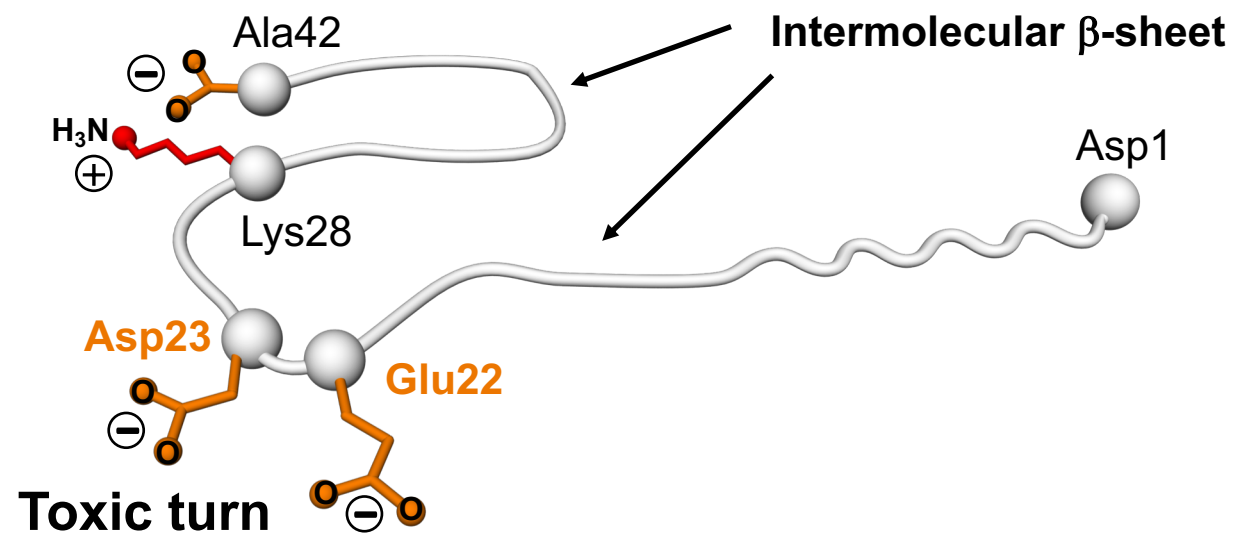


Figure 5

A β 42



A β 40

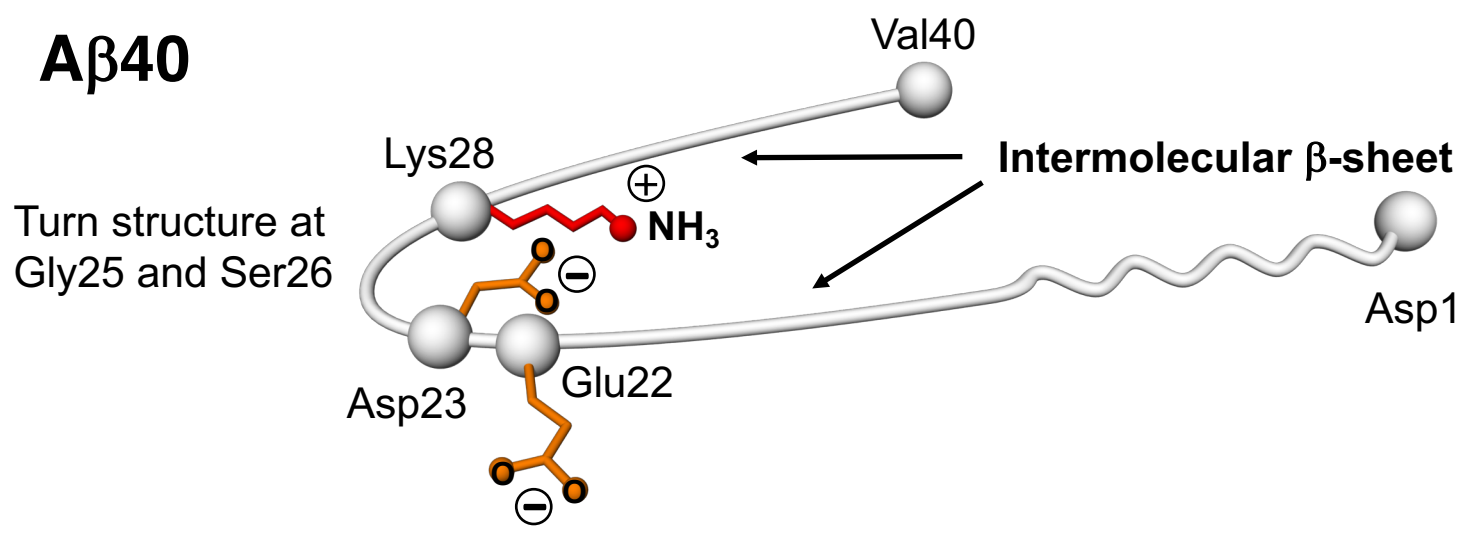


Figure 6

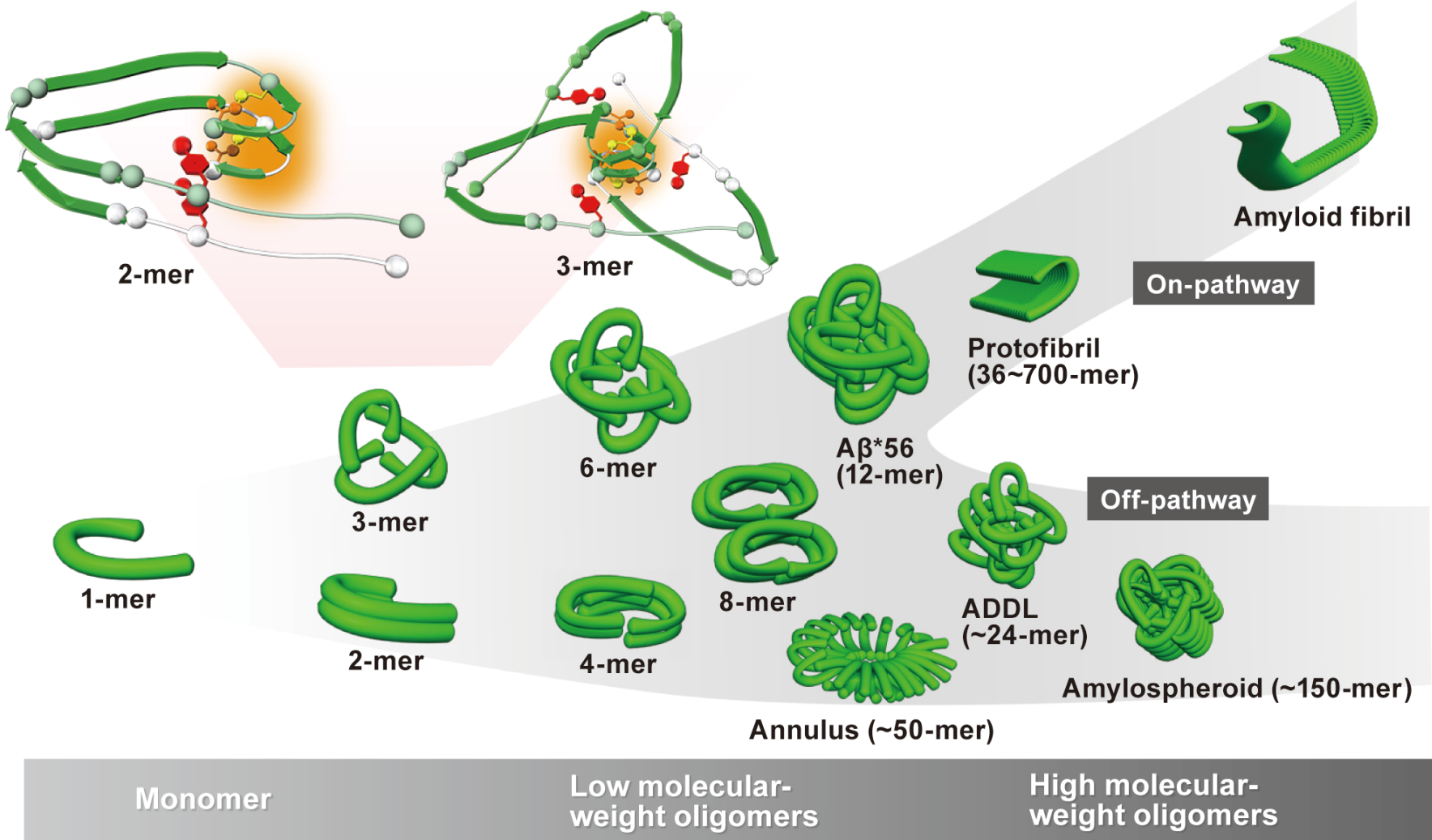
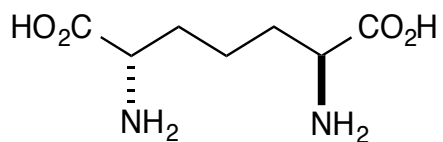
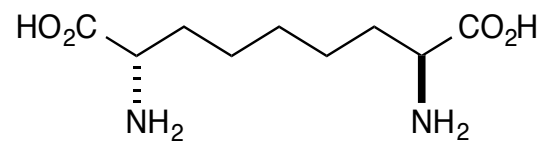


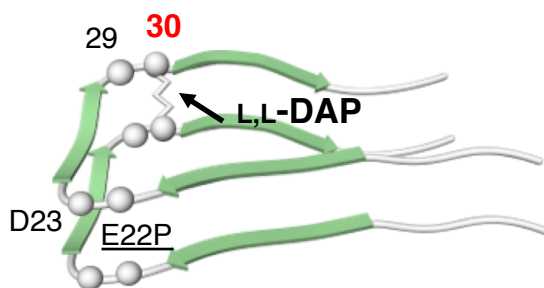
Figure 7



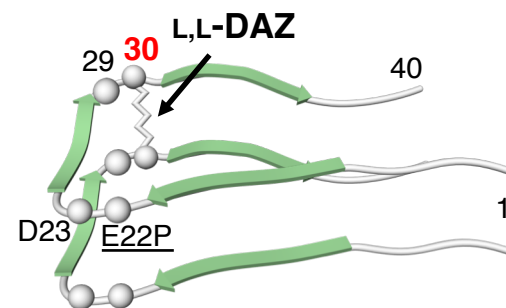
L,L-Diaminopimelic acid (DAP)



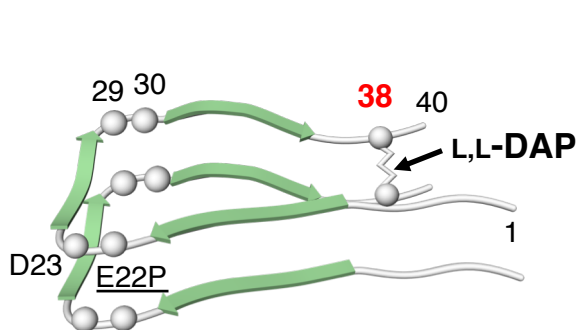
L,L-Diaminoazelaic acid (DAZ)



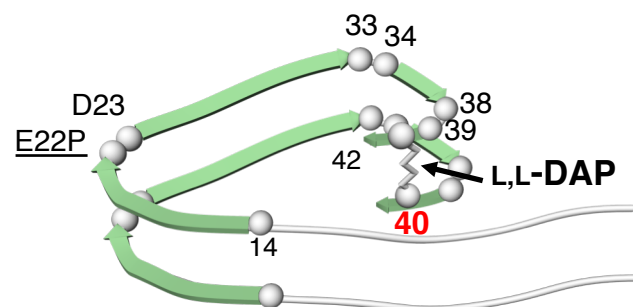
E22P,A30DAP-Aβ40 dimer (1)



E22P,A30DAZ-Aβ40 dimer (2)



E22P,G38DAP-Aβ40 dimer (3)



E22P,V40DAP-Aβ42 dimer (4)

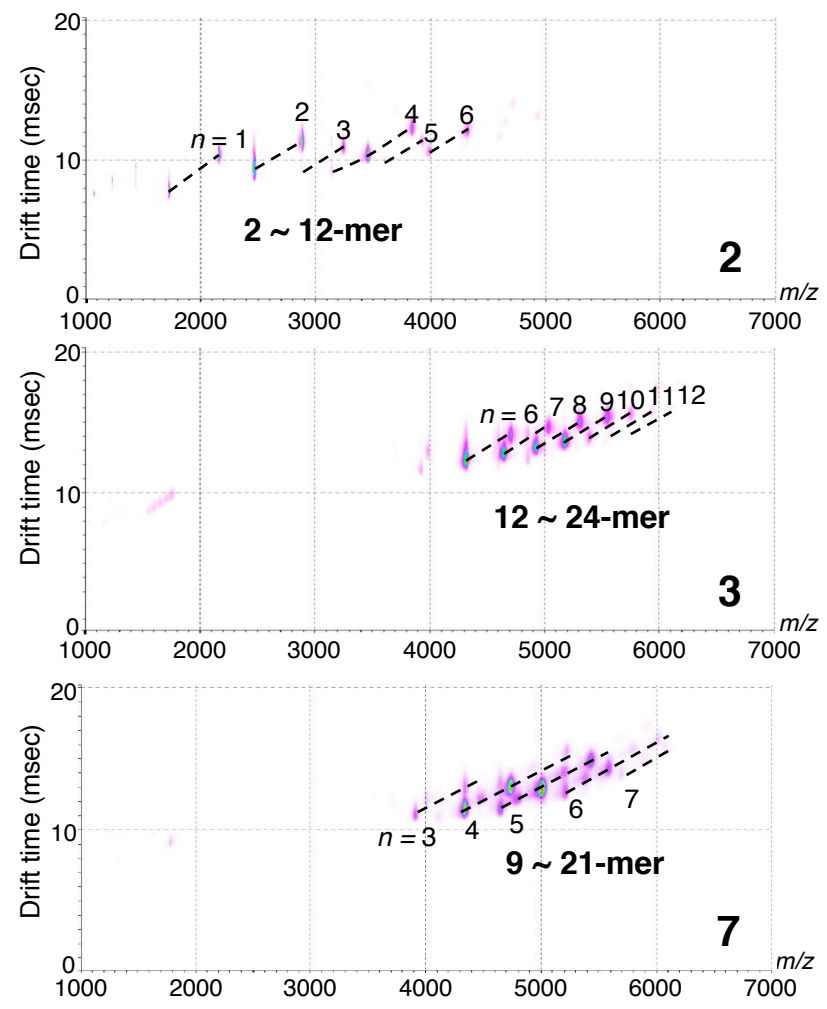
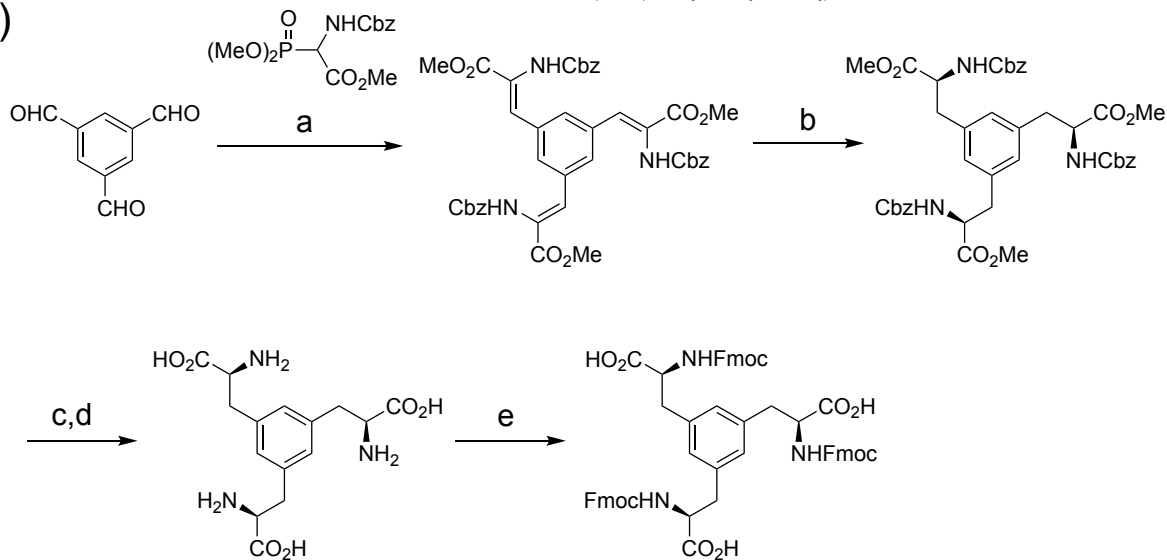
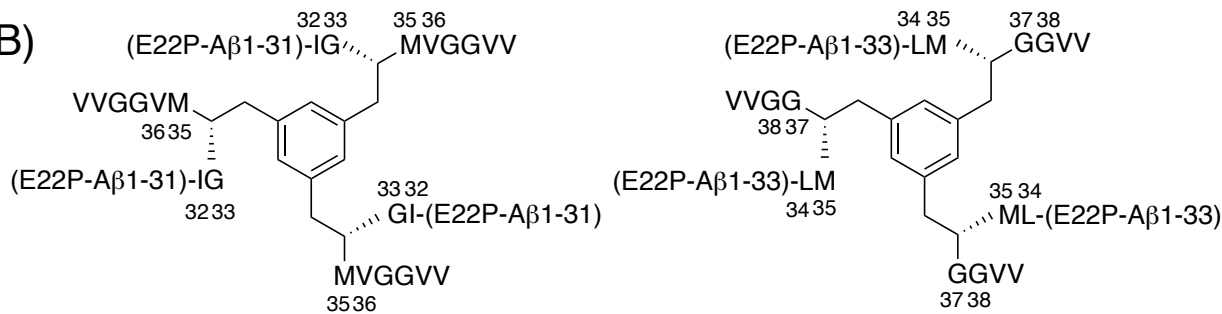


Figure 9

(A)

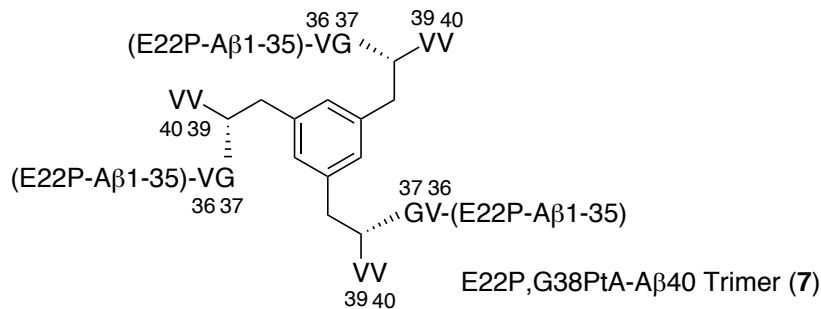


(B)



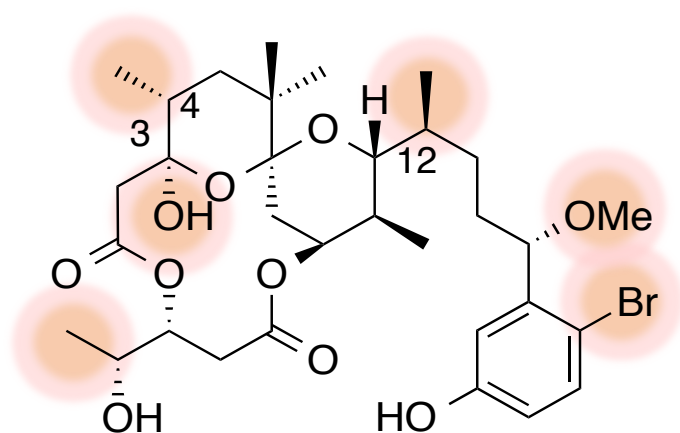
E22P,L34PtA-Aβ40 Trimer (5)

E22P,V36PtA-Aβ40 Trimer (6)

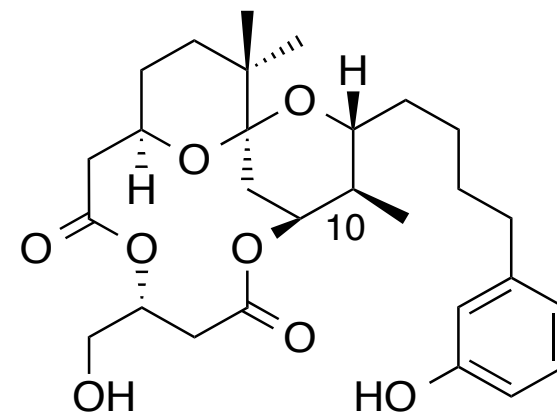


E22P,G38PtA-Aβ40 Trimer (7)

Figure 10



**Extraction of
anti-proliferative
activity**



“Master key”

Aplysiatoxin (ATX)

Tumor promoting
Proinflammatory

Potent PKC ligand
Anti-proliferative activity

High toxicity *in vivo*



“Special key”

10-Me-aplog-1

Non-tumor promoting
Non-proinflammatory

Potent PKC ligand
Anti-proliferative activity

Low toxicity *in vivo*